UC-401
LBL-27186 c.1
Preprint

Lawrence Berkeley Laboratory
UNIVERSITY OF CALIFORNIA

Materials & Chemical Sciences Division

RECEIVED
LAWRENCE
BERKELEY LABORATORY

SEP 27 1989

LIBRARY AND
DOCUMENTS SECTION

Submitted to Journal of Chemical Physics

State-selective Ionization of Nitrogen in the X $^2\Sigma_g^+$ $v^+ = 0$ and $v^+ = 1$ States by Two-colour (1 + 1) Photon Excitation Near Threshold

T. Trickl, E. Cromwell, Y.T. Lee, and A.H. Kung

May 1989

For Reference

Not to be taken from this room

LBL-27186 c.1

Prepared for the U.S. Department of Energy under Contract Number DE-AC03-76SF00098.

DISCLAIMER

This document was prepared as an account of work sponsored by the United States Government. While this document is believed to contain correct information, neither the United States Government nor any agency thereof, nor the Regents of the University of California, nor any of their employees, makes any warranty, express or implied, or assumes any legal responsibility for the accuracy, completeness, or usefulness of any information, apparatus, product, or process disclosed, or represents that its use would not infringe privately owned rights. Reference herein to any specific commercial product, process, or service by its trade name, trademark, manufacturer, or otherwise, does not necessarily constitute or imply its endorsement, recommendation, or favoring by the United States Government or any agency thereof, or the Regents of the University of California. The views and opinions of authors expressed herein do not necessarily state or reflect those of the United States Government or any agency thereof or the Regents of the University of California.

State-selective Ionization of Nitrogen in the X $^2\Sigma_g^+$ $v^+ = 0$ and $v^+ = 1$ States by Two-colour (1 + 1) Photon Excitation Near Threshold

T.Trickl[+], E.Cromwell, Y.T.Lee, A.H.Kung

Materials and Chemical Sciences Division, Lawrence Berkeley Laboratory, and Department of Chemistry, University of California, Berkeley, CA 94720

[+]Present address: Max-Planck-Institut für Extraterrestrische Physik, D 8046 Garching, Federal Republic of Germany

Abstract

Efficient generation of N_2^+ X $^2\Sigma_g^+$ ($v^+ = 0, 1$) is demonstrated by an extreme-ultraviolet + visible (1+1) photon excitation scheme. The c_4' $^1\Sigma_u^+$ ($v' = 0, 1$) Rydberg states are used as intermediates. The N_2 molecules are ionized near the $v^+ = 0$ and $v^+ = 1$ ionization thresholds. The autoionizing $nd\delta_g$ $^1\Delta_g$ Rydberg series with the rotational quantum numbers N = 4, 5 and 6 (in the limit of l uncoupling) are observed for the first time. Extrapolation of the N = 4 series yields an ionization energy of N_2 of 125666.959(67) cm^{-1}.

1. Introduction

Photoionization of molecules which are excited to a Rydberg state is an elegant method to prepare the resulting ions in a single vibrational state and a limited number of rotational levels. The selectivity is based on the similarity of the Rydberg and ionic potential energy surfaces. A near-ideal Franck-Condon overlap leads to conservation of the vibrational quantum number during the ionizing transition. Incorporated in an efficient resonance-enhanced multi-photon ionization (REMPI) scheme this technique may yield large numbers of well-characterized ions for ion beam scattering experiments under defined conditions.

The validity of a $\Delta v = 0$ propensity rule for ionization starting from excited states was demonstrated by Meek et al. in studies of toluene and benzene[1,2]. (2+1) and (3+1) REMPI via Rydberg states has been successfully applied to vibrational state selection of NO^+ [3], H_2^+ [4,5,6,7], N_2^+ (A $^2\Pi_u$) [8] and NH_3^+ [9]. Subsequently, the ion-molecule reactions of NH_3^+ (v) with D_2 and CH_4 were investigated by Conaway et al.[10,11].

The method, as used so far, does not have general applicability. This is mainly due to the limited wavelength range of the tunable laser sources employed and the often complicated electronic configurations of the Rydberg states involved. Each molecule requires a special excitation scheme. The rigid sequence of excitation frequencies determined by the choice of intermediate levels often leads to a high excess energy in the ionizing step. In addition, in many cases resonance-free two- or three-photon excitation is involved, which requires tight focussing of the laser in order to provide strong enough intensity for this nonlinear process to occur. Consequently, Coulomb repulsion in the small focal point due to space charge formation leads to temporal and spatial widening of the ion pulse. Severe loss of ions is observed for beams with sufficiently high currents for ion beam scattering experiments. Also, at these laser intensities, one has to consider absorption of additional photons by the ions.

With the advent of powerful laser-based vacuum-ultraviolet and extreme-ultraviolet (XUV) photon sources the REMPI method has gained substantial flexibility. Direct access to high-lying Rydberg levels becomes possible. With the choice of single-photon transitions for this step, focussing of the light beam into the gas becomes unnecessary. For two-colour (1+1) photon ionization, the wavelength of the second laser can be freely adjusted to values favourable for the state selection.

In an earlier experiment, we demonstrated very efficient (1+1) photon ionization of H_2 via the C $^1\Pi_u$ state[12]. The excess energy of the ionizing step is identical to that of one of the (3+1) photon experiments of Refs. 5, 6, 7, which verified the vibrational state-selection of the ion. In this paper, we report our first results on the more problematic case of N_2. The photoelectron spectra by Pratt et al. show good vibrational state selection for X $^2\Sigma_g^+$ in a (3+1) photon ionization process via c_3 $^1\Pi_u$ and c_4' $^1\Sigma_u^+$ [13]. There is, however, accompanying the production of strong population in the A $^2\Pi_u$ state of the ion. This process is, in principle, not very likely to occur because it requires a two-electron transition. The observation is therefore explained by the strong electronic mixing of the c and c′ states with states which allow formation of $N_2^+(A)$ in a single-electron transition[13]. Opitz et al. tried to avoid the formation of A state ions by reducing the excess energy to below the A state ionization threshold (9016.021(8) cm^{-1} [14]) [15]. This was achieved by using a two-colour (2+1+1) photon ionization scheme involving the $a^1\Pi_u$ (v = 4) and the c_3 or c_4' (v = 0) states as intermediates. With the resulting excess energy of $\Delta E \approx 7500$ cm^{-1}, however, they did not observe any ions at all though they obtained large quantities of two-colour ion signal for higher ΔE[15].

This result led us to reduce the excess energy significantly. In our experiment, we excited the c_4' (v′ = 0, 1) states directly with XUV light of 95.85 nm and 94.01 nm wavelength, respectively. The molecule was subsequently ionized near the X $^2\Sigma_g^+$ $v^+ = 0$ and $v^+ = 1$ thresholds with a second laser which was tuned around 468.5 nm and 465.7 nm, respectively. With this excitation scheme, we were able to create a substantial amount of state-selected N_2^+ ions.

2. Experimental

The experimental set-up has been described in detail elsewhere[16,17]. XUV light is generated by frequency tripling 25 to 30 mJ of the frequency-doubled output of a pulse-amplified continuous-wave ring dye laser (Coherent Radiation CR699-29 Autoscan; the three amplifier dye cells, operated with Rhodamine 610 and Rhodamine 590 dyes, are pumped by the second harmonic of a Quantel YG 592 laser) in a pulsed xenon beam[16]. The bandwidth of the XUV light slightly exceeds the minimum bandwidth of 210 MHz[16,17] with the xenon pressure adjusted for optimum power conversion. The slight broadening is caused by strong gas breakdown in the focus. Still, the recorded X → c_4' spectral lines were wider than the bandwidth. This is mainly due to residual Doppler broadening and the short upper state lifetime of 0.9 ns[18]. The ultraviolet light is removed from the XUV beam

by a 1 m normal incidence monochromator (McPherson, model 225). The curved grating re-focusses the beam which then intersects a differentially-pumped pulsed N_2 jet with a diameter of about 5 mm, 16 cm away from the nozzle. At this intersection, photoions are generated by a counterpropagating beam from a second dye laser (laser 2, Quanta Ray PDL, pumped by the third harmonic of a Quanta Ray DCR 2A Nd-YAG laser; the beam diameter of laser 2 was about 2 mm). The output of this laser, run with Coumarin 460 dye, was kept below 1 mJ. By this, the otherwise strong amplified spontaneous emission, which would cause a wavelength-independent ion signal, was suppressed. The ions were accelerated in a delayed, 23.6 V/cm pulsed extraction field to ensure field-free conditions during the ionization process. They were subsequently mass selected in a time-of-flight mass analyser and detected by a Daly detector equipped with a Johnston MM-1 multiplier. The signal was averaged with a boxcar integrator (Stanford Research Systems) and recorded with an IBM PC computer.

3. Results and Discussion

The spectral lines excited by the XUV light and their measured transition frequencies are listed in Table 1, along with line positions computed from literature values for comparison. Our numbers were determined using the Autoscan wavemeter which we had calibrated with I_2 reference lines[25] in a preceding experiment. Good agreement is obtained with the data calculated from revised a $\rightarrow$ X vibronic data[22] and the (0, 0) and (1, 0) bands of the $c_4' \rightarrow$ a transition[21] (column 4). We have also tried the X $\rightarrow$ c_3 (0, 0) transition as the first step in our (1+1) photon ionization scheme. This resulted in significantly smaller ion signal as could be expected from the smaller oscillator strength and the stronger predissociation of c_3 (0) compared with c_4' (0)[26]. The R and Q branch frequencies of this band are included in Table 1, as well as the (I_2-calibrated) R branch frequencies of the b$'$ $\rightarrow$ X (2, 0) band.

A selection of our two-colour spectra is given in Fig. 1. They were obtained by scanning laser 2 across the $v^+ = 0$ and $v^+ = 1$ thresholds, starting from c_4' $^1\Sigma_u^+$ v = 0 and v = 1, respectively. In all cases, a constant, structureless continuum is seen on the high-frequency side of the spectra. Below the threshold, the signal drops to zero, but exhibits a number of resonances which will be discussed below. We conclude, from the fact that the signal disappears on the low-energy side of the ionization limit for both, the $v^+ = 0$ and $v^+ = 1$ cases, that the ions in the continua are vibrationally state-selected. This is consistent with the expectations

derived from the photoelectron spectra by Pratt et al.[13].

The evidence of dominant direct ionization can also be seen from another measurement with c_4' ($v' = 0$, $J' = 0$) as intermediate level. By applying a continuous extraction field the $v^+ = 0$ ionization threshold can be shifted to the low-frequency side of the progression of resonances. There, we observed an onset the sharpness of which was limited by the bandwidth of laser 2 (0.5 cm^{-1}). Widening of the step would be expected in the presence of significant autoionization[27]. Thus, preparation of N_2^+ in a single rotational state might be possible.

By fitting a simple $\Delta\nu \sim \sqrt{E}$ model for the dependence of the frequency shift on the electric field[28,29] to our observed thresholds we obtain

$$\nu_{thr.}(\,E\,)\,[\,cm^{-1}\,] = 21340.54(56) - 5.55\sqrt{E\,[\,V/cm\,]} \quad (\,E \leq 100\ V/cm\,) \quad (1)$$

(for laser 2). The threshold values were taken at half-rise. From this equation and the (0, 0) R_0 frequency of Table 1 we calculate an ionization energy for N_2 of 125666.99(56) cm^{-1} which is close to the value given by Ogawa and Tanaka of 125666.8 cm^{-1} [30].

This excellent agreement suggests that the step observed at elevated field strength corresponds to ions in the $N_+ = 0$ rotational level. The $N_+ = 1$ and $N_+ = 2$ levels are distant by 3.84 cm^{-1} and 11.53 cm^{-1}, respectively[31], which is substantially greater than the uncertainties of the above extrapolation and Ogawa and Tanaka's ionization energy[30b] (see below). Theoretical considerations predict only even rotational levels to be populated by the $^1\Sigma_g^+$ ($J'' = 0$) $\rightarrow$ $^1\Sigma_u^+$ ($J' = 1$) $\rightarrow$ $^2\Sigma_g^+$ pathway, with the electron being ejected in an even partial wave[32]. This was confirmed by a very recent two-colour (2+1+1) REMPI study of N_2 by Fujii et al. with c_4' (v' = 0, J' = 5, 6) as final intermediate levels[33]. The selection rules for resonance-enhanced (n+1) photon ionization ($n \geq 0$), given by Dixit and McKoy[32], and/or a propensity rule for low angular momentum transfer in the ionizing step are verified by a number of REMPI and single-photon ionization experiments with rotational analysis of the photoions by high-resolution photoelectron spectroscopy[34 to 43] or laser-induced fluorescence[15,33]. Thus, we don't expect too many rotational levels of N_2^+ to be populated by our excitation scheme, especially when comparing the quite analogous case of the (3+1) photon ionization of H_2 via B $^1\Sigma_u^+$ [37]. In one of our spectra recorded in the presence of a continous extraction field there was some indication of a second step near the $N_+ = 2$ energy. However, this step needs to be confirmed by measurements with a better signal-to-noise ratio.

The ionization scheme presented in this paper is fairly efficient. Though the experimental parameters were not optimized we observed about 4×10^3 N_2^+ ions per laser shot with laser 1 tuned to $c_4' \leftarrow X\ (0, 0)R_0$ and laser 2 to 466.758 nm. Substantially more signal can be expected with higher pulse energy from laser 2 (the ionizing step is not saturated for ≤ 1 mJ) and from carefully matching the overlap of the two light beams and the gas beam (see Sec. 2). Further improvements can be achieved with higher frequency tripling efficiency for 95.85 nm [44], higher reflectivity of the XUV grating and with better ion transmission of the mass spectrometer. Also, for a powerful source of state-selected N_2^+ ions, one could greatly increase the N_2 density over our estimated density of just $1\times10^{13}\mathrm{cm}^{-3}$.

The Rydberg series observed in our spectra terminate in the region of a pair of discrete humps near the ionization limit under consideration ($v^+ = 0, 1$) in each of the four cases studied (i.e., $v' = 0$, $J' = 1, 2, 3$ and $v' = 1$, $J' = 1$ as the intermediate level). These broad humps, at first glance, seem to be formed by congestion due to the strong convergence of the spectral lines and should thus be close to the series limits. Fig. 2 shows an expanded section of the spectrum in Fig. 1a recorded with a resolution of one data point per 0.15 cm^{-1} (lower trace). The upper trace of Fig. 2 displays a neon reference spectrum. For the spectrum of Fig. 2, laser 2 was attenuated to about 10 μJ in order to minimize potential resonance-enhanced two-photon absorption. There is no N_2^+ energy level near the two-photon energy of laser 2 (the closest level is $A\ ^2\Pi_u\ v^+ = 7$ which is located about 159 cm^{-1} above it). In spite of the attenuation of laser 2 by two orders of magnitude the ratio of the hump and the continuum signals is still roughly the same as in Fig. 1a. This, together with the fact that there is no saturation-induced line broadening of more than 0.05 cm^{-1} observable in Fig. 1a, confirms the absence of two-photon effects. The ionization mechanism for the resonances must therefore be autoionization, or field-induced autoionization[45] for levels below the ionization threshold. These observations suggest that the Rydberg series converge to $v^+ = 0$ (or $v^+ = 1$ in the case of Fig. 1d). Convergence to higher vibrational levels is excluded by the large vibrational spacing ($\omega_e = 2207.0366 \pm 0.05\ \mathrm{cm}^{-1}$ [46]).

The Rydberg series converging towards $X\ ^2\Sigma_g^+$ that can be excited from the c_4' state are $ns\sigma_g\ ^1\Sigma_g^+$, $nd\sigma_g\ ^1\Sigma_g^+$ and $nd\pi_g\ ^1\Pi_g$, and, for $|\Delta\Lambda| > 1$, also $nd\delta_g\ ^1\Delta_g$ [47]. None of these series have been experimentally verified. The transitions to the $^1\Sigma_g^+$ states should exhibit P and R branches, those to the $^1\Pi_g$ states P, Q and R branches. In the case of l uncoupling[27,37,48,49,50] for the nd states, which becomes likely for high principal quantum numbers, the rotational quantum number N of

the "nd complexes" can only assume odd or even values. The correlation diagram for l uncoupling, i.e., the transition from Hund's case b to case d, is shown in Fig. 3. It is derived by considering the displayed sequence of electronic states and the non-crossing theorem for levels with equal J. For $J' = 1$ in the c_4' state as intermediate level application of the $|\Delta J| \leq 1$ selection rule yields N = 0, 2 and 4 as final levels, for $J' = 2$, N = 1, 3 and 5, and for $J' = 3$, N = 0, 2, 4 and 6. The final levels with $N = J' + 3$ belong to the $^1\Delta_g$ states and can be populated since for l uncoupling Λ is not defined any more. The individual Rydberg series correspond to certain values of N. They converge to the ionic rotational levels with the quantum numbers $N_+ = N$ [27]. The spin doublet splitting of the X $^2\Sigma_g^+$ state of N_2^+ is very small[31,51] and cannot be resolved in our experiment.

The spectrum of Fig. 2 shows essentially just one of the three series possible for J' = 1. This clarity facilitated the evaluation of the series limit. The results of the calculation are listed in Table 2 together with the measured transition frequencies. The series of Fig. 2 can be approximated by a simple Rydberg formula

$$\nu_n = \nu_\infty - \frac{R}{(n-\delta)^2}, \qquad R = 109735.17\ \mathrm{cm}^{-1}\ ^{52}, \tag{2}$$

for $50 \leq n \leq 74$ according to our assignment. A least-squares fit yields ν_∞ = 21378.952(22) cm^{-1} ($\pm$0.060 cm^{-1}, if one includes the calibration error) and δ = $-0.088(22)$. The agreement of the measured and calculated line positions is excellent. Typical differences lie within $\pm$0.05 cm^{-1} (i.e., one third of the minimum scan step of the PDL laser), and $\pm$0.10 cm^{-1} in the region away from xenon reference lines (see Fig. 2). The series is obviously free of major local perturbations in the analysed wavelength range.

The extrapolated series limit nearly coincides with the $N_+ = 4$ threshold calculated from the literature[30,31] and Table 1, 21378.793 cm^{-1}. It is, thus, evident that our series converges to $N_+ = 4$. According to the correlation diagram in Fig. 3 the series must be formed by the $nd\delta_g\ ^1\Delta_g$ states. The resulting ionization energy of N_2 is 125666.959(67) cm^{-1}.

For $J' = 2$ and 3 in the c_4' state as intermediate levels we see more complex spectra then for $J' = 1$ (see Figs. 1b, 1c). In spite of the higher number of spectral lines there is, once again, one particular Rydberg series dominating in both traces. As one goes from $J' = 1$ to $J' = 2$ and $J' = 3$ the spacing between neighbouring lines at a given frequency is getting wider, and in Fig. 1c one can follow the progression of lines even beyond the first broad hump. Extrapolation of the dominating series

of Figs. 1a, b, c by using Eq. 2 yields perfect agreement (i.e., $\pm 0.05 cm^{-1}$) with the $N_+ = 4, 5, 6$ thresholds, respectively, if one subtracts 0.73 cm^{-1} from each of the three series limits. Consequently, all these series are formed by $nd\delta_g\ ^1\Delta_g$ states.

The blueshift of 0.73 cm^{-1} may be due to a calibration change of laser 2. Also, Stark shift of the Rydberg states cannot be excluded since the spectra of Figs. 1 were taken with roughly 100 times higher intensity of laser 2 ($E \approx 4\times10^4$ V/cm) than that of Fig. 2.

The line positions are reproduced by the fits to within typically 0.1 cm^{-1} though many lines in Figs. 1b and 1c are rather broad or overlapping with others. The quantum defects are equal to within ± 0.02 of each other their value (–0.18) being slightly different from that derived from the neon-calibrated scan because the frequency offset changes by about 0.4 cm^{-1}across the scanning range.

The nature of the two broad humps which appear in all the spectra has to remain uncertain. If one considers merely congestion of the lines of the most intense, the $N = J' + 3$ series one would not expect more than one hump because the transition moments disappear as n^{-3} for hydrogen-like systems[53]. If one tries to assign the humps to two different series, the second series should correspond to $N = J' + 1$ because of the parity conservation in the autoionization process[48]. However, the frequency differences between the positions of the two humps and those of the $N_+ = J' + 1$ and $N_+ = J' + 3$ ionic levels (marked in Figs. 1) are not constant or even positive (see Figs. 1a, 1b). An explanation of the broad features by "accidental" resonances would be hard to believe since they occur at both, the $v^+ = 0$ and $v^+ = 1$ thresholds.

The answer can only be found from an experiment with substantially higher resolution. With better resolution, also, the $ns\sigma_g\ ^1\Sigma_g^+$, $nd\sigma_g\ ^1\Sigma_g^+$ and $nd\pi_g\ ^1\Pi_g$ Rydberg series may become observable and one might be able to detect the zero-field onset of the ionization continuum between the progressions of lines. Also, these measurements should yield a value for the ionization energy of N_2^+ improved by another order of magnitude.

Acknowledgements

This work was supported by the Director, Office of Energy Research, Office of Basic Energy Sciences, Chemical Sciences Division of the U.S. Department of Energy under contract no. DE-AC03-76SF00098.

References

1. J.T.Meek, S.R.Long, J.P.Reilly, J.Phys.Chem. 86 (1982) 2809 - 2811
2. S.R.Long, J.T.Meek, J.P.Reilly, J.Chem.Phys. 79 (1983) 3206 - 3219
3. J.C.Miller, R.N.Compton, Chem.Phys.Lett. 93 (1982) 453 - 459 (two-colour excitation)
4. S.L.Anderson, G.T.Kubiak, R.N.Zare, Chem.Phys.Lett. 105 (1984) 22 - 27
5. S.T.Pratt, P.M.Dehmer, J.L.Dehmer, Chem.Phys.Lett. 105 (1984) 28 - 33
6. S.T.Pratt, P.M.Dehmer, J.L.Dehmer, J.Chem.Phys. 85 (1986)3379 - 3385
7. M.A.O'Halloran, S.T.Pratt, P.M.Dehmer, J.L.Dehmer, J.Chem.Phys. 87 (1987) 3288 - 3298
8. S.T.Pratt, P.M.Dehmer, J.L.Dehmer, J.Chem.Phys. 80 (1984) 1706 - 1708
9. W.E.Conaway, R.J.S.Morrison, R.N.Zare, Chem.Phys.Lett. 113 (1985) 429 - 434
10. a) R.J.S.Morrison, W.E.Conaway, R.N.Zare, Chem.Phys.Lett. 113 (1985) 435 - 440

    b) R.J.S.Morrison, W.E.Conaway, T.Ebata, R.N.Zare, J.Chem.Phys. 84 (1986) 5527 - 5535
11. W.E.Conaway, T.Ebata, R.N.Zare, J.Chem.Phys. 87 (1987) 3447 - 3452
12. A.H.Kung, T.Trickl, N.A.Gershenfeld, Y.T.Lee, Chem.Phys.Lett. 144 (1988) 427 - 430
13. S.T.Pratt, P.M.Dehmer, J.L.Dehmer, J.Chem.Phys. 81 (1984) 3444 - 3451
14. W.Benesch, D.Rivers, J.Moore, J.Opt.Soc.Am. 70 (1980) 792 - 799
15. S.Opitz, D.Proch, T.Trickl, K.L.Kompa, to be published; a selection of the results was presented at the 1986 CLEO conference (book of abstracts, p. 72)
16. E.Cromwell, T.Trickl, Y.T.Lee, A.H.Kung, Ultra-Narrow Bandwidth XUV - VUV Laser System, to be published
17. T.Trickl, M.J.J.Vrakking, E.Cromwell, Y.T.Lee, A.H.Kung, Phys.Rev.A 39 (1989) 2948 -2955

18. J.E.Hesser, K.Dressler, J.Chem.Phys. 45 (1966) 3149 - 3150

19. P.K.Carroll, C.C.Collins, K.Yoshino, J.Phys.B 3 (1970) L127 - L131

20. J.Bendtsen, J.Raman Spectrosc. 2 (1974) 133 - 145

21. A.Lofthus, Can.J.Phys. 35 (1957) 216 - 234

22. D.Proch, T.Trickl, to be published

23. J.T.Vanderslice, S.G.Tilford, P.G.Wilkinson, Astrophys.J. 141 (1965) 395 - 426

24. a) Band origin: K.Yoshino, private communication in Ref. 47

b) Rotational constants: A.Lofthus, Can.J.Phys. 35 (1957) 216 - 234, Table XII: Ref. "Janin(1950)"; we use the rotational constant B_c for the Q branch and B_d for the R branch, which minimizes the discrepancies.

25. a) S.Gerstenkorn, P.Luc, Atlas du Spectre d'Absorption de la Molécule d'Iode (14800 - 20000 cm^{-1}), Éditions du Centre National de la Recherche Scientifique (1978)

b) Correction of - 0.0056 cm^{-1} taken from: S.Gerstenkorn, P.Luc, Revue Phys. Appl. 14 (1979) 791 - 794

26. E.C.Zipf, R.W.McLaughlin, Planet.Space Sci. 26 (1978) 449 - 462

27. W.A.Chupka, J.Berkowitz, J.Chem.Phys. 51 (1969) 4244 - 4268

28. H.A.Bethe, E.E.Salpeter, Quantum Mechanics of One- and Two-Electron Atoms, Springer-Verlag (1957)

29. a) W.E.Cooke, T.F.Gallagher, Phys.Rev.A 17 (1978) 1226 - 1228 ;

b) T.F.Gallagher, L.M.Humphrey, W.E.Cooke, R.M.Hill, S.A.Edelstein, Phys.Rev.A 16 (1977) 1098 - 1108

30. a) M.Ogawa, Y.Tanaka, Can.J.Phys. 40 (1962) 1593 - 1607

b) Ogawa and Tanaka do not give an error limit for their measurements. The measured and calculated numbers in Table 1 of Ref. 30a differ typically by less than 0.5 cm^{-1}.

31. T.A.Miller, T.Suzuki, E.Hirota, J.Chem.Phys. 80 (1984) 4671 - 4678

32. S.N.Dixit, V.McKoy, Chem.Phys.Lett. 128 (1986) 49 - 54

33. A.Fujii, T.Ebata, M.Ito, J.Chem.Phys. 88 (1988) 5307 - 5313

34. L.Åsbrink, Chem.Phys.Lett. 7 (1970) 549 - 552

35. Y.Morioka, S.Hara, M.Nakamura, Phys.Rev.A 22 (1980) 177 - 182

36. J.E.Pollard, D.J.Trevor, J.E.Reutt, Y.T.Lee, D.A.Shirley, J.Chem.Phys. 77 (1982) 34 - 46

37. S.T.Pratt, P.M.Dehmer, J.L.Dehmer, J.Chem.Phys. 78 (1982) 4315 - 4320

38. W.G.Wilson, K.S.Viswanathan, E.Sekreta, J.P.Reilly, J.Phys.Chem. 88 (1984) 672 - 673

39. K.Müller-Dethlefs, M.Sander, E.W.Schlag, Z.Naturforsch. 39*a* (1984) 1089- 1091

40. K.Müller-Dethlefs, M.Sander, E.W.Schlag, Chem.Phys.Lett. 112 (1984) 291 - 294

41. K.S.Viswanathan, E.Sekreta, E.R.Davidson, J.P.Reilly, J.Phys.Chem. 90 (1986) 5078 - 5084

42. M.Sander, L.A.Chewter, K.Müller-Dethlefs, E.W.Schlag, Phys.Rev.A 36 (1987) 4543 - 4546

43. W.Habenicht, R.Baumann, K.Müller-Dethlefs, E.W.Schlag, Ber.Bunsenges. Phys.Chem. 92 (1988) 414 - 416

44. The efficiency at this wavelength is rather low with the most commonly used tripling gases; see: R.H.Page, R.J.Larkin, A.H.Kung, Y.R.Shen, Y.T.Lee, Rev.Sci.Instrum. 58 (1987) 1616 - 1620

45. E.Y.Xu, H.Helm, R.Kachru, Phys.Rev.A 38 (1988) 1666 - 1669, and references therein

46. R.A.Gottscho, R.W.Field, K.A.Dick, W.Benesch, J.Mol.Spectrosc. 74 (1979) 435 - 455

47. A.Lofthus, P.H.Krupenie, J.Phys.Chem.Ref.Data. 6 (1977) 113 - 307

48. G.Herzberg, Molecular Spectra and Molecular Structure, I. Spectra of Diatomic Molecules, 2^{nd}Ed., van Nostrand (1950)

49. P.M.Dehmer, W.A.Chupka, J.Chem.Phys. 65 (1976) 2243 - 2273

50. S.Fredin, D.Gauyacq, M.Horani, C.Jungen, G.Lefèvre, Mol.Phys. 60 (1987) 825 - 866

51. S.D.Rosner, T.D.Gaily, R.A.Holt, J.Mol.Spectrosc. 109 (1985) 73 - 84

52. Mass-corrected value, using R_∞ from: F.Biraben, J.C.Garreau, L.Julien, M.Allegrini, Phys.Rev.Lett. 62 (1989) 621 - 624

53. See e.g. J.Berkowitz, Photoabsorption, Photoionization and Photoelectron Spectroscopy, Accademic Press (1979)

Figure Captions

Fig. 1

(1+1) photon ionization spectra recorded by scanning laser 2 across the $v^+ = 0$ and $v^+ = 1$ thresholds; laser 1 is tuned to the

a) (0, 0) R_0
b) (0, 0) R_1
c) (0, 0) R_2
d) (1, 0) R_0

lines of the $c_4' \leftarrow X$ transition of N_2. The ion signal is not corrected for the intensity changes of the two light beams. The N_2^+ rotational level positions are marked as calculated from the literature[20,30,31,46] and Table 1.

Fig. 2

Lower trace: Section of the spectrum in Fig. 1a recorded with maximum scan resolution of laser 2; the ion signal is divided by the XUV power. The fluctuations are mostly due to boxcar baseline drifts. N_2^+ level positions are marked as taken from the literature[30,31,46] and Table 1. The assignment of the Rydberg states is derived from fits of Eq. 2 to the measured frequencies.

Upper trace: Neon reference spectrum; four of the calibration lines are identified for convenience

Fig. 3

Correlation diagram of the transition from Hund's case b to Hund's d for an nd complex

Table 1

Comparison of N_2 Transition Frequencies from this Work and from Previous Spectroscopic Studies (All Entries in cm^{-1})

Transition		This Work$^+$	Other Work	
$c_4' \rightarrow X$ (0,0)	R_0	104326.451(25)	104327.16^a	104326.32(20)^b
	R_1	104330.190(25)	104330.89^a	104330.08(20)^b
	R_2	104333.802(25)	104334.51^a	104333.68(20)^b
$c_4' \rightarrow X$ (1,0)	R_0	106372.005(35)	106372.92^a	106371.84(20)^b
	R_1	106374.849(35)	106375.79^a	106374.62(20)^b
$c_3 \rightarrow X$ (0,0)	R_0	104141.506(35)	104141.17^c	
	R_1	104143.461(35)	104143.14^c	
	R_2	104144.361(35)	104144.09^c	
	Q_1	104137.592(35)	104137.22^c	
	Q_2	104135.644(35)	104135.27^c	
$b' \rightarrow X$ (2,0)	R_0	105153.440(15)	105153.88^d	
	R_0	105154.047(15)	105154.47^d	
	R_2	105152.963(25)	105153.37^d	

$^+$ These numbers were determined in a one-laser 1 + 1 photon ionization experiment with the monochromator set to 0th order. Frequency corrections were carried out as described in Ref. 17.

^{a} Calculated from band origins from Ref. 19 and rotational constants from Refs. 20 and 21

^{b} Calculated from $c_4' \rightarrow a$ (0, 0) line positions from Ref. 21, the $a \rightarrow X$ (0, 0) band origin from Ref. 22, and rotational constants from Refs. 20 and 23

^{c} Calculated from molecular constants of Refs. 20 and 24

^{d} Calculated from molecular constants of Ref. 19

Table 2

List of the Frequencies of the Transitions Excited from the c_4' (0) $J' = 1$ Level (All Frequencies in cm^{-1})

n	$\nu_{meas.}$	$\nu_{calc.}$(Equ.2)	Difference
50	21335.260	21335.212	+0.048
51	21336.895	21336.908	−0.013
52	21338.528	21338.507	+0.021
53	21340.057	21340.016	+0.041
54	21341.395	21341.442	−0.047
55	21342.826	21342.792	+0.034
56	21344.012	21344.070	−0.058
57	21345.285	21345.281	+0.004
58	21346.323	21346.430	−0.107
59	21347.441	21347.522	−0.081
60	21348.510	21348.559	−0.049
61	21349.538	21349.546	−0.008
62	21350.481	21350.486	−0.005
63	21351.405	21351.381	+0.024
64	21352.228	21352.235	−0.007
65	21353.045	21353.049	−0.004
66	21353.856	21353.827	+0.029
67	21354.545	21354.571	−0.026
68	21355.298	21355.282	+0.016
69	21355.998	21355.962	+0.036
70	21356.590	21356.613	−0.023
71	21357.226	21357.237	−0.011
72	21357.903	21357.836	+0.067
73	21358.463	21358.410	+0.053
74	21358.923	21358.960	−0.037
∞		21378.952(22)	

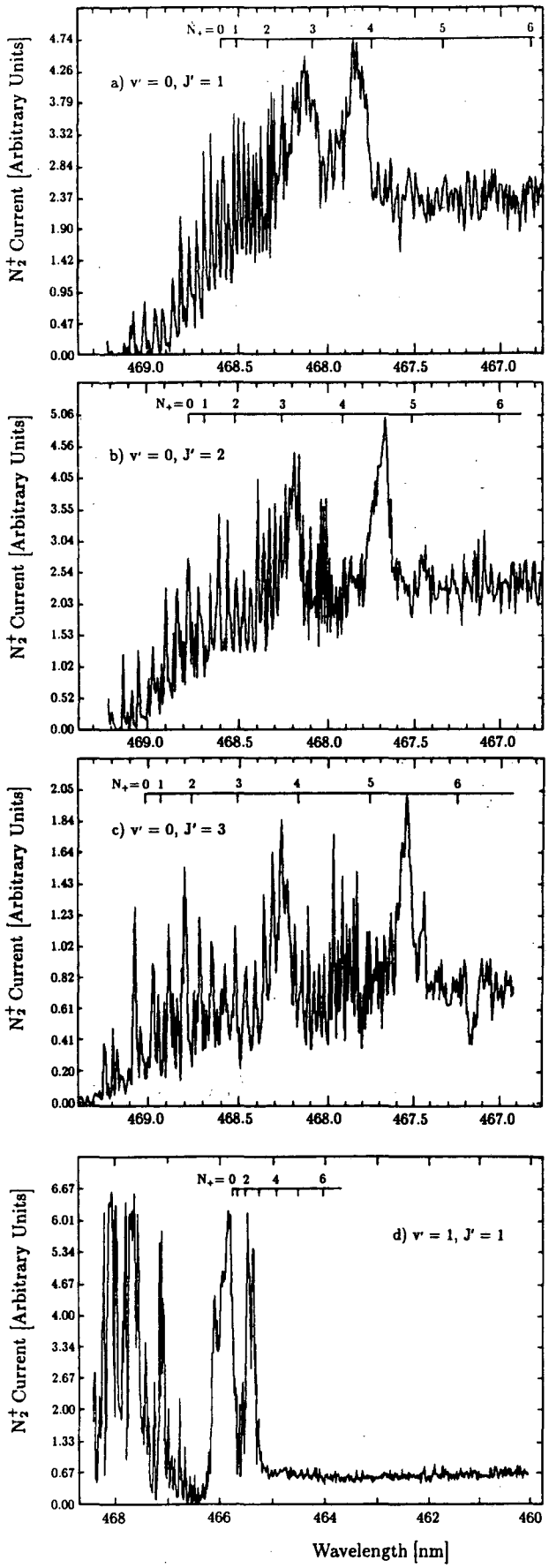

Trickl et al.

Fig. 1

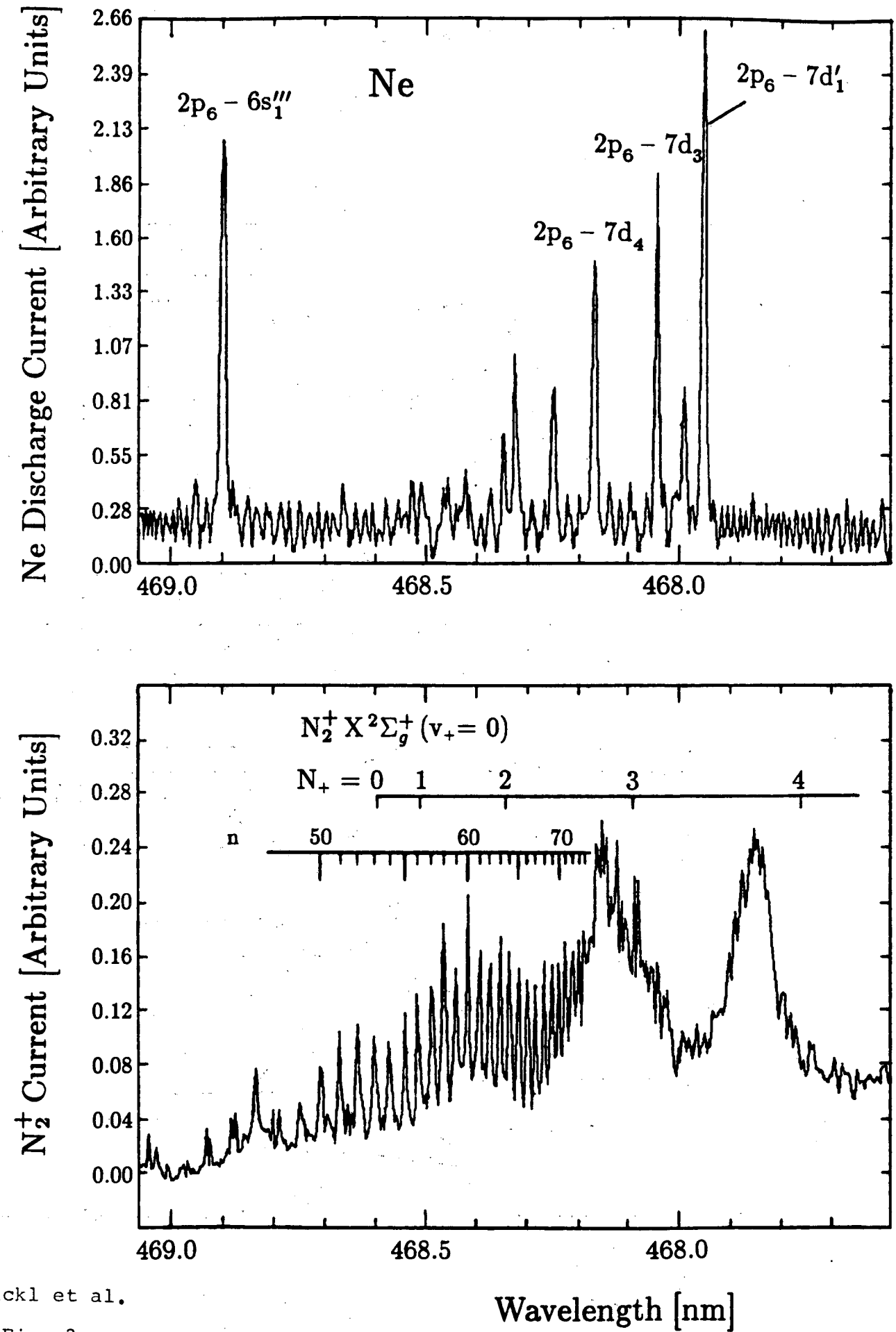

Trickl et al.

Fig. 2

Fig. 3

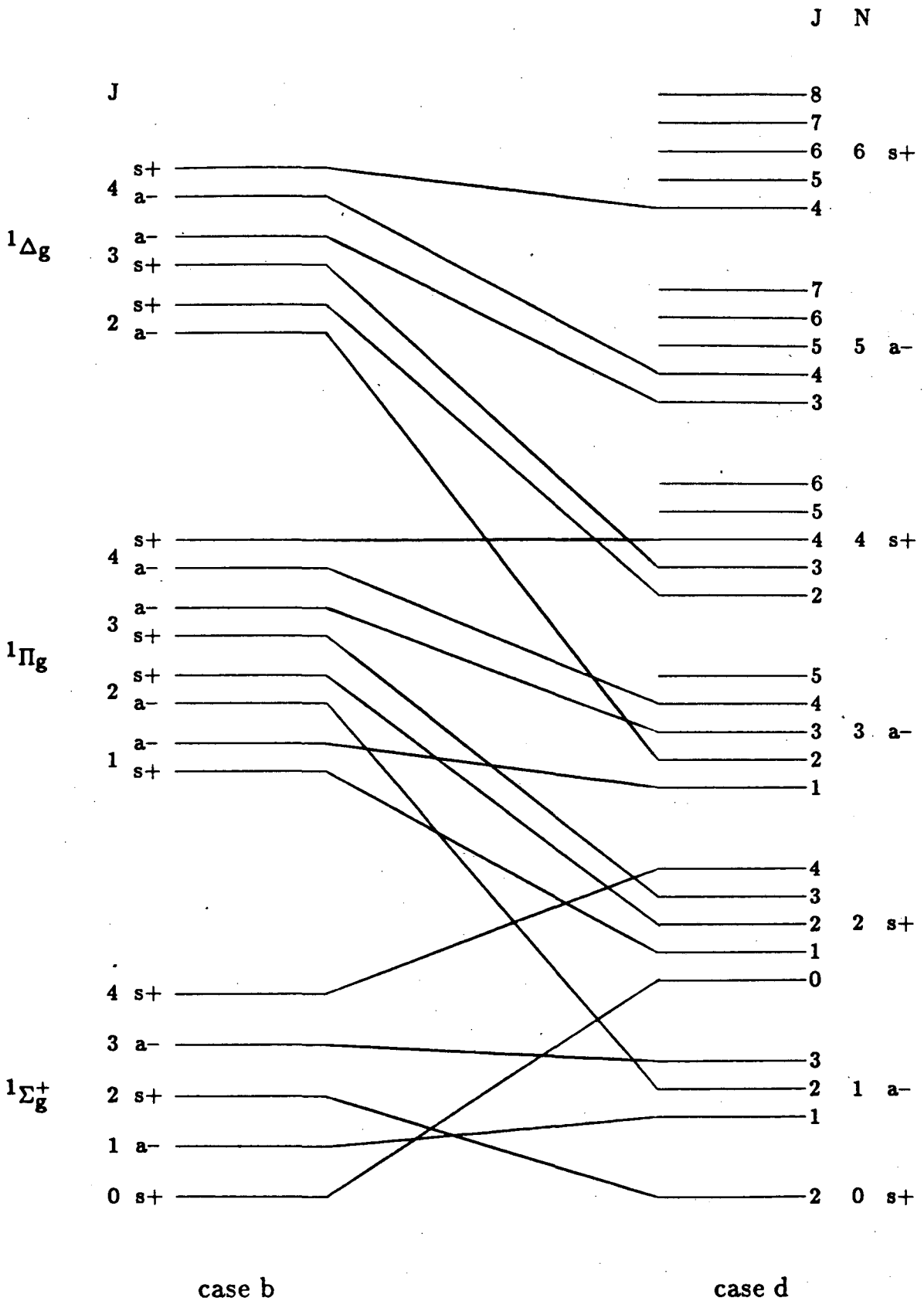
J
N
J
$^1\Delta_g$
$^1\Pi_g$
$^1\Sigma_g^+$
4 s+
4 a−
3 a−
3 s+
2 s+
2 a−
4 s+
4 a−
3 a−
3 s+
2 s+
2 a−
1 a−
1 s+
4 s+
3 a−
2 s+
1 a−
0 s+
8
7
6
5
4
7
6
5
4
3
6
5
4
3
2
5
4
3
2
1
4
3
2
1
0
3
2
1
2
6 s+
5 a−
4 s+
3 a−
2 s+
1 a−
0 s+
case b
case d

LAWRENCE BERKELEY LABORATORY
TECHNICAL INFORMATION DEPARTMENT
1 CYCLOTRON ROAD
BERKELEY, CALIFORNIA 94720